RSC Advances

RSC Publishing

COMMUNICATION

View Article Online
View Journal | View Issue

Facile method for the environmentally friendly fabrication of reduced graphene oxide films assisted by a metal substrate and saline solution†

Cite this: *RSC Advances*, 2013, **3**, 14286

Received 22nd April 2013,
Accepted 5th July 2013

DOI: 10.1039/c3ra41984c

www.rsc.org/advances

Seonuk Park,[a] Sooji Nam,[a] Jihun Hwang,[a] Jaeyoung Jang,[a] Tae Kyu An,[a] Jiye Kim,[a] Yebyeol Kim,[a] Se Hyun Kim,*[b] Dae Sung Chung*[c] and Chan Eon Park*[a]

In this study, a graphene oxide film supported on a steel sheet was prepared by electrophoretic deposition and then treated with a NaCl solution to form a reduced graphene oxide (rGO) film. The rGO film displayed an electrical conductivity of 40.7 S m^{-1}, and was prepared using benign and environmentally friendly reduction conditions.

Graphene is a two-dimensional carbon allotrope, one atom thick, that displays excellent mechanical, thermal, and electrical properties. Graphene oxide (GO), a sheet comprising highly oxidized graphite, and reduced graphene oxide (rGO), a chemical derivative of graphene, has attracted considerable interest in recent years because its solution processability renders the material amenable to a variety of fabrication processes and their applications.[1–6]

GO is usually reduced *via* a chemical reaction with N_2H_4, $NaBH_4$, NaOH, KOH, HI, and hydroquinone.[7–13] Unfortunately, these methods are harmful, and the use of these agents requires great care. The high temperature (~1000 °C) reduction of GO under argon or an argon/hydrogen gas mix has been used to prepare high-quality rGO; however, these methods require the consumption of large amounts of energy.[8,10,14]

Recent efforts have attempted to identify a green and low-energy substitute for the above methods of preparing rGO, such as alcohol[15] or cellulose[16] as reducing agents. Among them, non-toxic metal with an appropriate reductive capacity, such as Fe or Zn, are attractive candidates for the development of eco-friendly reduction processing approaches.[17–20] Previous reduction processes developed using metal powders have required the addition of an acid or a base to facilitate the oxidation reaction. Appropriate nontoxic modifications to these metal-assisted reduction reactions are needed for the environmentally friendly production of rGO.

The use of rGO in large-scale applications demands that the rGO dispersion stability be prioritized. The unique properties of graphene are mainly available only when rGO takes the form of individual sheets, and most applications of rGO have required dispersal in a solvent. Unfortunately, rGO formed using metal-assisted reduction methods tend to form irreversible agglomerates.[17–19] Several strategies for reducing GO films have been proposed in an effort to address the dispersion problems associated with rGO preparation, including vaporization of a reducing agent (N_2H_4, HI) in the presence of the GO film,[8,12] reduction of the GO film by palladium chloride ($PdCl_2$) in a pressurized hydrogen system,[21] or UV irradiation of a titanium oxide–graphene oxide composite film[22,23] or a GO-polyoxometalate composite film.[24]

Here, we prepared a GO film supported on a steel sheet under electrophoresis, which is a standard method used in the preparation of films from a solution. The electrophoretically deposited GO (EPD-GO) film was then exposed to a sodium chloride (NaCl) solution to reduce the graphene oxide film. Steel sheets more are readily oxidized in the presence of a NaCl solution than in the presence of water due to the greater conductivity of the electrolytes in solution.[25] The NaCl solution, therefore, increases the rate of the reduction–oxidation (redox) reaction between the steel sheet and the GO.

GO was deposited by electrophoretic deposition onto the steel sheet. The wet EPD-GO film supported on steel sheet was dried overnight in ambient air to remove any residual water. The dried EPD-GO film mounted on the steel sheet was then exposed to a NaCl solution (5 wt% NaCl in deionized water) by spraying at 35 °C for 1 h. The NaCl solution-treated EPD-GO film mounted on a steel sheet was denoted an "EPD-rGO film".

The top photograph in Fig. 1 shows that the color of the thin EPD-GO film supported on a steel sheet changed after exposure to a NaCl solution. The color of the EPD-GO film turned from brown to black, suggesting the formation of rGO. The color change upon exposure to the NaCl solution was more rapid than the color changed observed upon exposure to deionized water, as shown in

[a]*POSTECH Organic Electronics Laboratory, Polymer Research Institute, Department of Chemical Engineering, Pohang University of Science and Technology, Pohang 790-784, Korea. E-mail: cep@postech.ac.kr; Fax: +82-54-279-8298; Tel: +82-54-279-2269*
[b]*Department of Advanced Organic Materials Engineering, Yeungnam University, 280 Daehak-ro, Gyeongsan, 712-749, Korea. E-mail: shkim97@yu.ac.kr; Fax: +82-53-810-4686; Tel: +82-53-810-2778*
[c]*School of Chemical Engineering and Material Science, Chung Ang University, Seoul, Republic of Korea. E-mail: dchung@cau.ac.kr; Fax: +82-2-820-8375; Tel: +82-2-820-5270*

† Electronic supplementary information (ESI) available: Experimental procedures, photograph, XRD patterns and TGA plots. See DOI: 10.1039/c3ra41984c

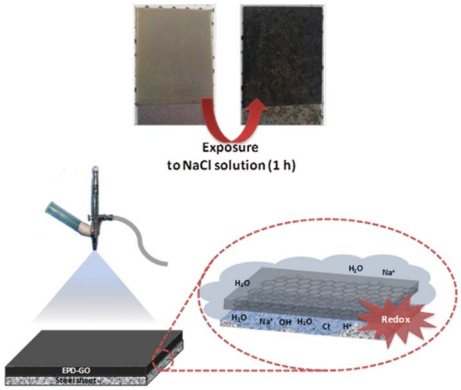

Fig. 1 Optical photographs of an EPD-GO thin film and an EPD-rGO thin film supported on a steel sheet (top), and schematic diagram of the redox reaction between an EPD-GO film and a steel sheet in the presence of a NaCl solution (bottom).

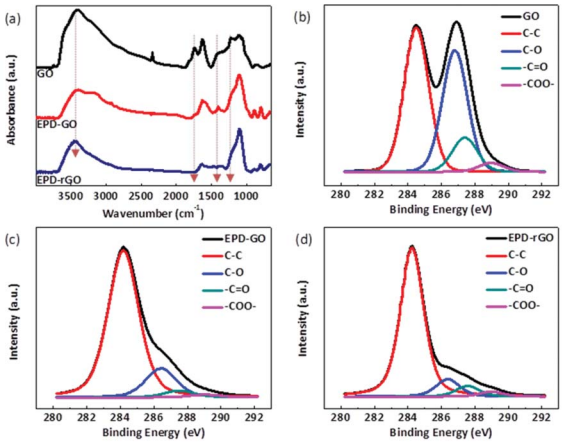

Fig. 3 (a) FT-IR spectra of the GO, EPD-GO, and EPD-rGO dispersed in KBr pellets, and (b) C 1s XPS spectra of the GO paper, (c) EPD-GO film, and (d) EPD-rGO film.

Fig. 1 and Fig. S1, ESI.† The color changes and relative rates of the color changes pointed toward a redox reaction between the steel sheet and the EPD-GO film that was facilitated by the NaCl solution (lower panel in Fig. 1).

Cross-sectional images of the EPD-GO and EPD-rGO films were collected by scanning electron microscopy (SEM, S-4800, Hitachi) with a view toward surveying the microscopic changes that occurred in the films. The platelets in the EPD-GO film were loosely stacked, whereas the rGO platelets in the EPD-rGO film were more tightly packed (Fig. 2). This observation was consistent with the theta-2 theta mode out-of-plane X-ray diffraction (XRD, 8D beamline at Pohang Accelerator Laboratory, λ = 1.813 Å) patterns, as shown in Fig. S2, ESI.† A broad rocking curve in the case of EPD-GO was shifted toward large angles and became sharper after exposure to the NaCl solution. These observations were attributed to the removal of intercalated water molecules from the layer interstices, and to the removal of certain oxygen-containing functional groups, such as hydroxy, epoxy, ether, ketone, and carboxylic acid groups, from the platelets in the EPD-GO film. The close packing between the rGO platelets and the narrowing of the interlayer spacing also provided evidence supporting the effective reduction of the EPD-GO film.

Differences among the oxygen-containing functional groups in the EPD-GO and EPD-rGO may be clearly observed in the Fourier transform infrared spectra (FT-IR, Nicolet 6700, Thermo Elec. Co.) and in the X-ray photoemission spectra (XPS, 4D beamline at the Pohang Accelerator Laboratory). The EPD-GO and EPD-rGO films could be easily peeled from the steel sheets, and the FT-IR samples could be prepared by dispersing the materials in KBr pellets. As the GO was processed to form EPD-rGO, the intensities of the absorption peaks related to the oxygen functional groups decreased, as shown in Fig. 3(a). The intensities of the absorption peaks (dotted lines) corresponding to stretching (3430 cm^{-1}) and bending vibrations (1410 cm^{-1}) among the hydroxyl groups (–OH) in GO and the water molecules, the stretching vibration (1734 cm^{-1}) of the carbonyl groups (C=O) in the carboxylic acid derivatives, and the C–O stretching vibration (1223 cm^{-1}) in the phenolic groups, significantly decreased as the processing sequence progressed. The trend observed in the FT-IR spectra corresponded to the results obtained from the C 1s XPS spectra. As shown in Fig. 3(b), 3(c), 3(d), the intensities of the highest binding energy peaks, including the peaks centered at 286.7 eV (C–O), 287.8 eV (–C=O), and 288.8 eV (–COO–), gradually decreased as GO was processed to form EPD-rGO on a steel sheet. The intensities of the GO, EPD-GO, and EPD-rGO, peaks centered at 284.5 eV (C–C) did not change significantly. The FT-IR and XPS results suggest that the oxygen-containing functional groups were removed and the conjugated graphene networks were restored after each processing step.

The thermal stabilities of the GO, EPD-GO, and EPD-rGO films were measured by thermogravimetric analysis (TGA, TGA 2050, TA instruments), as shown in Fig. 4. The GO curve revealed a

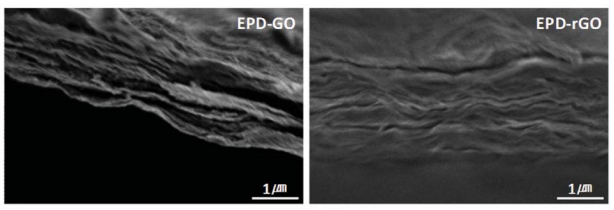

Fig. 2 SEM cross-sectional images of the EPD-GO and EPD-rGO films.

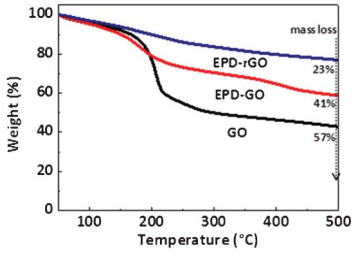

Fig. 4 Normalized TGA plots of the GO powder, EPD-GO film, and EPD-rGO film.

Table 1 Conductivity of the GO paper, EPD-GO and EPD-rGO films

	GO (30 um)[a]	EPD-GO (10 um)[a]	EPD-rGO (10 um)[a]
Conductivity (S m^{-1})	Insulator	0.58 (172.4)[b]	2.7 (37.05)[b]

[a] Thickness of paper and films. [b] Sheet resistance (KΩ sq^{-1}).

significant mass loss around 200 °C due to pyrolysis of the unstable oxygen-containing functional groups. Compared to the 57 wt% mass loss at 500 °C in the GO sample, the mass losses in the EPD-GO and EPD-rGO samples were 41 and 23 wt%, respectively. These results suggest that the EPD-rGO film was the most thermally stable film because the oxygen-containing functional groups of the EPD-rGO film were fewer than in the GO and EPD-GO films. The EPD-rGO film appeared to be the most extensively reduced among the films, after the post-processing step. Interestingly, the mass loss of the EPD-GO film prepared by dipping in a stirred hydrazine hydrate solution (1 wt%) at 100 °C for 6 h was 25 wt%, as shown in Fig. S3, ESI,† indicating that the reduction by Fe/NaCl was as effective as the reduction by the hydrazine hydrate solution.

The SEM, XRD, FT-IR, XPS, and TGA results indicated that the EPD-rGO film was significantly reduced during exposure to the NaCl solution. The redox reaction under the NaCl solution post-processing step may be expressed as follows:[17,18]

$$M \longrightarrow M^{2+} + 2e^{-} \quad (M = Fe, Zn) \tag{1}$$

$$GO + aH^{+} + be^{-} \longrightarrow rGO + cH_2O \tag{2}$$

The oxidation (1) and reduction (2) reactions took place at the Fe and GO regions, respectively. Given that the conductivity of a salt solution is higher than the conductivity of the same solution without the salt, for a given pH, the corrosive current between the Fe and GO regions was expected to increase in the NaCl solution, thereby facilitating the transport of electrons generated in the Fe region to the GO region.[25]

Both electrophoretic deposition and exposure of the EPD-GO film supported on the steel sheet to the NaCl solution facilitated reduction. A previous report suggested that reduction of GO by electrophoretic deposition could be attributed to the electrochemical decarboxylation of GO.[26]

The electrical conductivities of the GO, EPD-GO, and EPD-rGO films were investigated to examine the state of the conjugated network in the EPD-rGO film, as determined by measuring the sheet resistance (CMT-SR200N, AIT) of the GO paper, the EPD-GO film, and the EPD-rGO films separated from the steel substrates (Table 1). As the number of oxygen-containing functional groups decreased, the conductivity was found to increase. The sheet resistance of the GO paper before and after exposure to the NaCl solution were nearly identical, indicating that the NaCl solution did not affect the conductivity of the GO or the reduction of GO in the absence of the steel substrate. The conductivity of the EPD-rGO film increased from 2.7 S m^{-1} to 40.7 S m^{-1} upon exposure of the supported EPD-GO film to NaCl solution for 2 h, indicating that the supported EPD-GO film was further reduced in the presence of the NaCl solution. The applicability of the NaCl solution method to other metals was tested by carrying out the preparation steps on a galvanized steel sheet (a steel sheet that has been coated with zinc *via* hot dipping) in place of the steel sheet. Surprisingly, the electrical conductivity of the EPD-rGO film supported on the galvanized steel sheets after exposure to the NaCl solution for 2 h was 62.9 S m^{-1}. The increased electrical conductivity observed in the case of the galvanized steel sheet resulted from the redox reaction between the Zn and EPD-GO in accordance with the electrochemical reaction described in eqn (1) and (2). The conductivity of the EPD-rGO film supported on the galvanized steel sheet was larger than the conductivity of the EPD-rGO film supported on the steel sheet because zinc is oxidized more readily than iron (zinc has more negative standard reduction potential (E°) than iron; E° of Zn/Zn^{2+} and Fe/Fe^{2+} are −0.762 V and −0.44 V, respectively).

In conclusion, a new reductive processing method was developed in which EPD-GO films supported on a steel sheet were exposed to a NaCl solution. An rGO film was fabricated using an environmentally friendly and nontoxic method without the need for acids, bases, or any other organic materials. Our post-processing reduction method did not result in dispersion problems in solution.

This work was supported by the National Research Foundation of Korea (NRF) grant funded by the Korea government (MSIP) (NRF-2009-0079630). We thank Hyojung Cha and Yong Jin Jeong for helpful discussions.

Notes and references

1 S. Park and R. S. Ruoff, *Nat. Nanotechnol.*, 2009, **4**, 217–224.
2 Y. Zhu, S. Murali, W. Cai, X. Li, J. W. Suk, J. R. Potts and R. S. Ruoff, *Adv. Mater.*, 2010, **22**, 3906–3924.
3 K. P. Loh, Q. Bao, G. Eda and M. Chhowalla, *Nat. Chem.*, 2010, **2**, 1015–1024.
4 E. Stratakis, M. M. Stylianakis, E. Koudoumas and E. Kymakis, *Nanoscale*, 2013, **5**, 4144.
5 P. Matyba, H. Yamaguchi, M. Chhowalla, N. D. Robinson and L. Edman, *ACS Nano*, 2011, **5**, 574–580.
6 C. Petridis, Y.-H. Lin, K. Savva, G. Eda, E. Kymakis, T. D. Anthopoulos and E. Stratakis, *Appl. Phys. Lett.*, 2013, **102**, 093115.
7 S. Stankovich, D. A. Dikin, R. D. Piner, K. A. Kohlhaas, A. Kleinhammes, Y. Jia, Y. Wu, S. T. Nguyen and R. S. Ruoff, *Carbon*, 2007, **45**, 1558–1565.
8 D. Yang, A. Velamakanni, G. Bozoklu, S. Park, M. Stoller, R. D. Piner, S. Stankovich, I. Jung, D. A. Field, C. A. Ventrice Jr and R. S. Ruoff, *Carbon*, 2009, **47**, 145–152.
9 Y. Si and E. T. Samulski, *Nano Lett.*, 2008, **8**, 1679–1682.

10 D. Luo, G. Zhang, J. Liu and X. Sun, *J. Phys. Chem. C*, 2011, **115**, 11327–11335.
11 S. Park, J. An, R. D. Piner, I. Jung, D. Yang, A. Velamakanni, S. T. Nguyen and R. S. Ruoff, *Chem. Mater.*, 2008, **20**, 6592–6594.
12 I. K. Moon, J. Lee, R. S. Ruoff and H. Lee, *Nat. Commun.*, 2010, **1**, 73.
13 G. Wang, J. Yang, J. Park, X. Gou, B. Wang, H. Liu and J. Yao, *J. Phys. Chem. C*, 2008, **112**, 8192–8195.
14 H. C. Schniepp, J.-L. Li, M. J. McAllister, H. Sai, M. Herrera-Alonso, D. H. Adamson, R. K. Prud'homme, R. Car, D. A. Saville and I. A. Aksay, *J. Phys. Chem. B*, 2006, **110**, 8535–8539.
15 D. R. Dreyer, S. Murali, Y. Zhu, R. S. Ruoff and C. W. Bielawski, *J. Mater. Chem.*, 2011, **21**, 3443–3447.
16 H. Peng, L. Meng, L. Niu and Q. Lu, *J. Phys. Chem. C*, 2012, **116**, 16294–16299.
17 Z. J. Fan, W. Kai, J. Yan, T. Wei, L. J. Zhi, J. Feng, Y. M. Ren, L. P. Song and F. Wei, *ACS Nano*, 2011, **5**, 191–198.
18 X. Mei and J. Ouyang, *Carbon*, 2011, **49**, 5389–5397.
19 Y. Liu, Y. Li, M. Zhong, Y. Yang, W. Yuefang and M. Wang, *J. Mater. Chem.*, 2011, **21**, 15449–15455.
20 S. Yang, W. Yue, D. Huang, C. Chen, H. Lin and X. Yang, *RSC Adv.*, 2012, **2**, 8827–8832.
21 J. Wang, M. Liang, Y. Fang, T. Qiu, J. Zhang and L. Zhi, *Adv. Mater.*, 2012, **24**, 2874–2878.
22 B. Li, X. Zhang, X. Li, L. Wang, R. Han, B. Liu, W. Zheng, X. Li and Y. Liu, *Chem. Commun.*, 2010, **46**, 3499–3501.
23 K. K. Manga, Y. Zhou, Y. Yan and K. P. Loh, *Adv. Funct. Mater.*, 2009, **19**, 3638–3643.
24 H. Li, S. Pang, S. Wu, X. Feng, K. Muüllen and C. Bubeck, *J. Am. Chem. Soc.*, 2011, **133**, 9423–9429.
25 D. A. Jones, *Principles and Prevention of Corrosion*, 2nd edn, Prentice Hall, Inc., 1996.
26 S. J. An, Y. W. Zhu, S. H. Lee, M. D. Stoller, T. Emilsson, S. Park, A. Velamakanni, J. H. An and R. S. Ruoff, *J. Phys. Chem. Lett.*, 2010, **1**, 1259–1263.